Large Magnetoresistance Oscillations in Mesoscopic Superconductors due to Current-Excited Moving Vortices

G. R. Berdiyorov,[1] M. V. Milošević,[1] M. L. Latimer,[2,3] Z. L. Xiao,[2,3,*] W. K. Kwok,[2] and F. M. Peeters[1,†]

[1]Departement Fysica, Universiteit Antwerpen, Groenenborgerlaan 171, B-2020 Antwerpen, Belgium
[2]Materials Science Division, Argonne National Laboratory, Argonne, Illinois 60439, USA
[3]Department of Physics, Northern Illinois University, DeKalb, Illinois 60115, USA

(Received 27 January 2012; published 31 July 2012)

We show in the case of a superconducting Nb ladder that a mesoscopic superconductor typically exhibits magnetoresistance oscillations whose amplitude and temperature dependence are different from those stemming from the Little-Parks effect. We demonstrate that these large resistance oscillations (as well as the monotonic background on which they are superimposed) are due to current-excited moving vortices, where the applied current in competition with the oscillating Meissner currents imposes or removes the barriers for vortex motion in an increasing magnetic field. Because of the ever present current in transport measurements, this effect should be considered in parallel with the Little-Parks effect in low-critical temperature (T_c) samples, as well as with recently proposed thermal activation of dissipative vortex-antivortex pairs in high-T_c samples.

DOI: 10.1103/PhysRevLett.109.057004 PACS numbers: 74.78.Na, 74.25.F−, 74.25.N−, 74.40.Gh

The circulation of electrons and Cooper pairs in doubly and multiply connected normal and superconducting materials in the presence of a magnetic field produces, respectively, the Aharonov-Bohm [1] and the Little-Parks (LP) effect [2]. These effects are sensitive probes for the proposed incoherent Cooper pairing in the pseudogap [3] and for insulating phases [4] competing with superconductivity in copper oxide and conventional superconductors, for the relative contribution of individual bands in two-band superconductors [5] and for the interplay of superconductivity and magnetism in hybrid structures [6]. They are expected to shed light on the d-wave symmetry [7] and the strip structures [8] in high temperature superconductors. Magnetoresistance oscillations have been widely observed in doubly and multiply connected mesoscopic superconductors [9–16] and have mostly been attributed to the LP effect, which is related to the periodic suppression of the critical temperature T_c due to fluxoid quantization [17,18]. However, analysis of magnetoresistance oscillations in recent experiments on high-T_c superconducting loops (in a specifically designed network), showed that neither the amplitude of the oscillations nor their temperature dependence could be explained by the LP effect [15]. In order to describe the experimental data, the authors used the fluxoid dynamics model [16], according to which thermally excited vortices-antivortices move and interact with the magnetic field-induced persistent currents.

Here, we present results of numerical simulations and transport measurements, which reveal a new origin for the magnetoresistance oscillations in mesoscopic superconductors, namely, the motion of current-excited vortices. These vortices are not excited by thermal fluctuations in contrast to the case of Refs. [15,16]. Instead, the applied current interacts with existing Meissner currents in the sample and tunes the barrier for vortex entry and exit while simultaneously driving the vortices. In addition, the ubiquitous monotonic background of the magnetoresistance curves is also found to be due to moving vortices. Since an external current is inherent to all transport measurements, the proposed mechanism needs to be considered in the studies of singly (stripes), doubly (loops), or multiply (ladders and wire networks) connected mesoscopic superconductors.

In what follows, we demonstrate our findings for a Nb ladder structure (i.e., a thin strip with a chain of holes, see Fig. 1), which is a transition geometry from a finite ring structures to an infinite network [19]. In this geometry, the electrical contact issues on the resistance, known to occur in individual loops [20], are suppressed. The choice of material and geometry was made to maximize the larger characteristic length scales to avoid the formation of "effective" weak links, which can result in direct superconducting-insulator transitions [21] and, consequently, large magnetoresistance oscillations in a broad range of temperatures and magnetic fields [22]. Finally,

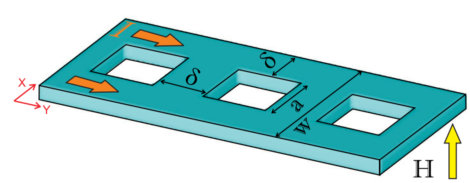

FIG. 1 (color online). An oblique view of the system: a superconducting strip (of width $w = a + 2\delta$, thickness $t \ll \lambda, \xi$, and periodically long in the y direction) with a chain of holes (size a and period $d = a + \delta$) under applied dc current I and a perpendicular magnetic field H.

thermal fluctuations in Nb are far less important than in high-T_c samples, which is also relevant for the analysis of our findings in comparison with Ref. [15].

Theory.—For the theoretical study of the fluxoid quantization and dynamics, we used the generalized time-dependent Ginzburg-Landau (GL) equations [23]

$$\frac{u}{\sqrt{1+\gamma^2|\psi|^2}}\left(\frac{\partial}{\partial t}+\frac{\gamma^2}{2}\frac{\partial|\psi|^2}{\partial t}\right)\psi = (\nabla - i\mathbf{A})^2\psi + (1 - T - |\psi|^2)\psi + \chi(\mathbf{r}, t), \quad (1)$$

$$\frac{\partial \mathbf{A}}{\partial t} = \mathrm{Re}[\psi^*(-i\nabla - \mathbf{A})\psi] - \kappa^2 \mathrm{rot\,rot}\mathbf{A}, \quad (2)$$

with the following units: the coherence length $\xi(0)$ for the distance, $t_{\mathrm{GL}}(0) = \pi\hbar/8k_B T_c u$ for time, T_c for temperature, and $\phi_0/2\pi\xi(0)$ for the vector potential $\mathbf{A}$. Order parameter ψ is scaled to its value for zero magnetic field and temperature, and the current density is in units of $j_0 = \sigma_n\hbar/2et_{\mathrm{GL}}(0)\xi(0)$. The material parameters $\gamma = 20$ and $u = 5.79$ follow from microscopic theory [23]. $\chi(\mathbf{r}, t)$ is the random fluctuating term [24]. To account for heating effects, we couple Eqs. (1) and (2) to the heat transfer equation (see Ref. [20] for details):

$$\nu\frac{\partial T}{\partial t} = \zeta\nabla^2 T + \left(\frac{\partial \mathbf{A}}{\partial t}\right)^2 - \eta(T - T_0), \quad (3)$$

where T_0 is the bath temperature. Here we use $\nu = 0.03$, $\zeta = 0.06$ and $\eta = 2\times 10^{-4}$, corresponding to an intermediate heat removal to the substrate [20]. The above equations are solved self-consistently using the semi-implicit Crank-Nicholson algorithm [25] with periodic boundary conditions in the y direction and Neumann boundary conditions at all sample edges. The transport current is introduced via the boundary condition for the vector potential rot $\mathbf{A}|_z(x = 0, w) = H \pm H_I$, where $H_I = 2\pi I/c$ is the magnetic field induced by the current I.

As a representative example, we studied the response to an external magnetic field of a superconducting strip of width $w = 40\xi(0)$ and with holes of size $a = 20\xi(0)$. Figure 2(a) shows the time averaged energy F (see Ref. [26] for the definition of F) of this system as a function of magnetic field for different values of the applied dc current I. For small current values (curve 1), the vortex entries are shifted to lower magnetic field compared to the case of no applied current (not shown here). Still, vortex entry remains a first-order transition; i.e., one observes a sharp drop in the energy at the transition field [indicated by a solid black arrow in Fig. 2(a). However, for the same current at larger magnetic fields we surprisingly found that vortex entry is characterized by a continuous change in energy, manifested by a second-order transition (dashed blue arrow). It is exactly these transitions that give rise to the large voltage signal $V = -\int \partial\mathbf{A}/\partial t \cdot d\mathbf{l}$, as shown in Fig. 2(b) (see curve 1). Such vortex entries are found at lower fields for larger applied current [curves 2 in

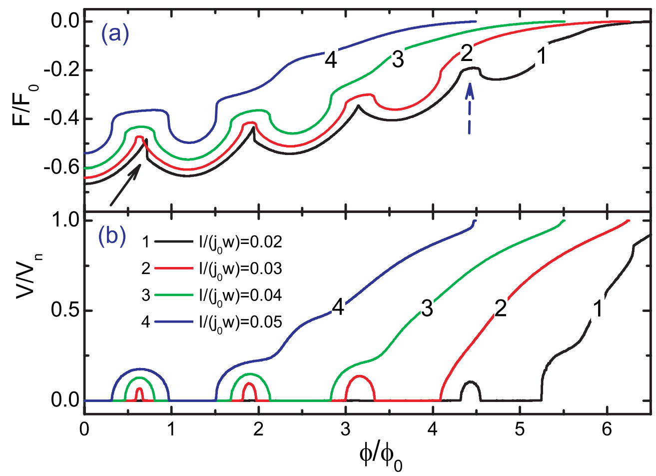

FIG. 2 (color online). Time-averaged free energy F (a) (in units of $F_0 = H_c^2 V_0/8\pi$ with V_0 the unit cell volume) and voltage V (b) (in units of normal state voltage V_n) as a function of external flux ϕ [calculated over the unit cell area $S = w \times (a + \delta)$] for different values of applied current I. The width of the simulated ladder is $w = 40\xi(0)$, and the size of the holes is $a = 20\xi(0)$. The temperature is $T = 0.98T_c$, and the GL parameter is $\kappa = 10$.

Fig. 2(a)]. With further increasing I, the magnetic fields at which voltage oscillations are located do not change, but oscillations become broader [curves 3 and 4 in Fig. 2(b)]. Note that oscillations in our curves are not exactly periodic with field and larger flux is needed to observe the first voltage peak (a typical effect for finite-walled ring structures, see, e.g., Ref. [11]).

To gain further insight into the process leading to magnetoresistance peaks, we plot the temporal voltage signal for $I/(j_0 w) = 0.04$ and $\phi = 0.64\phi_0$ in Fig. 3. At this field (i.e., just after the maximum of the first voltage peak), the output voltage oscillates periodically in time with a global minimum (point 1 in Fig. 3) corresponding to one vortex trapped inside the hole (inset 1). With time, this vortex exits the sample (inset 2) exhibiting a maximum in the $V(t)$ characteristics (point 2), and the system is free of vortices (inset 3). Immediately after, a new vortex penetrates the sample (inset 4), and the entire vortex entry-exit sequence repeats (see Ref. [27] for an animated data for this process).

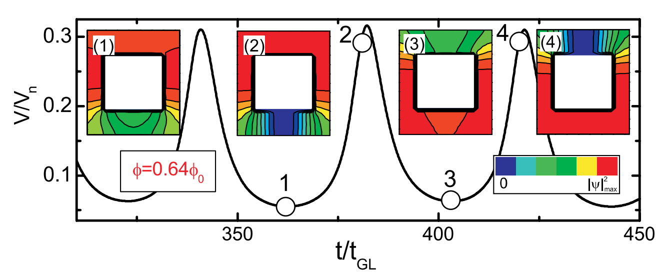

FIG. 3 (color online). Voltage vs time response for the sample of Fig. 2 for $\phi = 0.64\phi_0$ and $I/(j_0 w) = 0.04$. Insets show snapshots of $|\psi|^2$ at time intervals indicated by open circles on the $V(t)$ curves.

We stress once more that vortices in our study cannot be induced by thermal fluctuations, making our predictions different from ones in Refs. [15,16]. Note also that no voltage or resistance oscillations with time are expected from the LP effect, which is also different from our findings. The origin of vortex excitation in our system is the interplay of currents. Namely, applied magnetic field induces reactive screening (and circulating) currents in the superconductor, j_s. Therefore, applied dc current always enhances the supercurrent j_s on one side of the sample, while suppressing j_s on the other side. This directly affects the barriers for vortex entry and exit, which are indicated in Figs. 4(a) and 4(b), where we plotted the time evolution of the free energy of the system. When the total current $j_t = j_s + j$ reaches to its critical value [28] in one arm of the ladder, a vortex nucleates at the edge of the sample in spite of the finite energy barrier ΔF_p [see filled circles in Fig. 4(c)]. At that field, the barrier for the vortex expulsion ΔF_e on the opposite side of the sample is strongly suppressed [see open circles in Fig. 4(c)], since $j_t = j_s - j$. Therefore, the vortex is driven through the system resulting in periodic-in-time voltage signal as shown in Fig. 3. With further increasing the applied field, the barrier for vortex exit increases [open circles in Fig. 4(c)]. Consequently, the vortex remains trapped in the sample and the voltage becomes zero. Such modulation of the barrier for vortex entry and exit is observed for the transition between different vortex states [see the second voltage peak in Fig. 4(c)].

Thus, we conclude that each voltage (and magnetoresistance) peaks as a function of magnetic field corresponds to the moving vortices in the system, the motion of which is manipulated by the interplay of applied and Meissner currents. Note, however, that at higher driving current or for larger vorticity it is no longer possible to stabilize the stationary vortex state, and vortices always remain in motion, creating a background voltage (characteristic of a resistive state) on which the peaks for every additional vortex entry are superimposed [see curve 4 in Fig. 2(b)]. For this case, animated data for the evolution of the superconducting condensate with time, together with the corresponding voltage signal, are shown in the Supplemental Material [27]. The background on which the magnetoresistance oscillations are superimposed has been puzzling scientists since the original experiment of Little and Parks [2]. Several possible explanations have been put forth, including the Meissner effect, misalignment of the external field, and different single-particle excitation energies within an electron pair. Recently, Sochnikov *et al.* proposed an alternative mechanism which is based on thermally excited vortices and antivortices [15]. In our case, the background stems solely from the continuous, dissipative vortex motion.

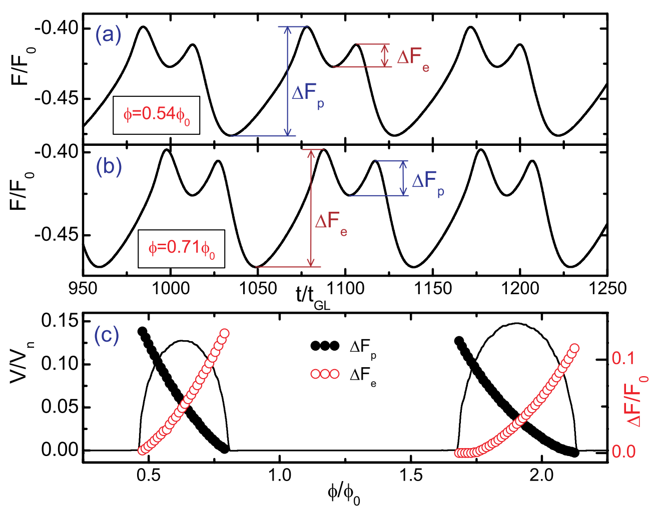

FIG. 4 (color online). (a),(b) Time evolution of the free energy for the ladder considered in Fig. 2 at $\phi = 0.54\phi_0$ (a) and $\phi = 0.71\phi_0$ (b). Arrows indicate the penetration ΔF_p and expulsion ΔF_e barriers. (c) Time-averaged voltage (solid curve), ΔF_p (filled circles), and ΔF_e (open circles) as a function of external flux. The applied current is $I/(j_0 w) = 0.04$.

Experiment.—In order to confirm our theoretical prediction, we performed magnetoresistance measurements on 100 nm thick Nb strips with a chain of square holes patterned with focused-ion-beam milling (see Ref. [29] for the details of sample fabrication and measurements). We considered Nb strips with width $w = 385$ nm, hole size $a = 120$ nm, and period $d = 300$, 385, and 800 nm. Magnetoresistance of the samples was obtained by four-probe dc measurements using a constant current mode. Here we present the results for the sample with interhole spacing $d = 385$ nm [see the lower inset in Fig. 5(b)], which shows a broad superconducting-normal transition with $T_c \approx 7.725$ K [using the criterion of 90% of the normal state resistance, see Fig. 5(b)]. Zero temperature coherence length $\xi(0)$ and the penetration depth $\lambda(0)$ were estimated to be 10 and 200 nm, respectively.

Figure 5(a) shows experimentally measured magnetoresistance curves of the sample at different temperatures (see Supplemental Material [30] for the results obtained for the sample with $d = 300$ nm). Because of the small bias current ($I = 1$ μA and current density $j = 2.5 \times 10^3$ A $\cdot$ cm^{-2}), no resistance oscillations are observed until higher temperatures ($T = 7.3$ K), where a first resistance peak appears at around 1400 Oe. Figure 5(c) shows the $R(H)$ curves obtained at $T = 7.42$ K for different values of the biased current. As delineated in this figure, the amplitude of the resistance oscillations is strongly affected by the bias current: the oscillations disappear both at larger and smaller currents. However, the position of the resistance peaks is independent of the applied current, as we predicted in our numerical simulations [see Fig. 2(b)].

We now analyze the amplitude of the resistance oscillations as a function of temperature, shown in the top inset of Fig. 5(b) by solid dots for the first peak of the $R(H)$ curves of Fig. 5(a). Open dots in this figure show the expected amplitude of the LP oscillations due to periodic changes in the superconducting transition temperature:

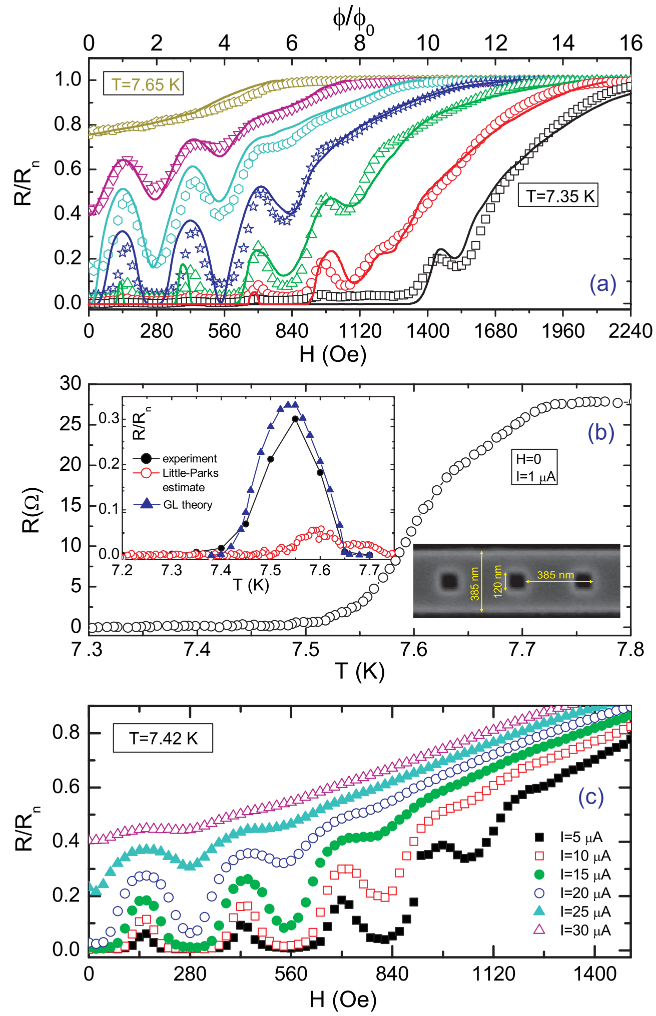

FIG. 5 (color online). (a) Measured resistance (in units of normal state resistance $R_n = 27.9\ \Omega$) vs magnetic field for a Nb superconducting strip (of width $w = 385$ nm) with a chain of holes (of size $a = 120$ nm and period $d = 385$ nm) in applied dc current $I = 1\ \mu$A and at different temperatures (ranging from $T = 7.35$ K to $T = 7.65$ K with step 50 mK). Solid curves show theoretical results for the dimensions of the experimental sample and for $I/(j_0 w) = 0.05$. (b) $R(T)$ curve of the sample at zero magnetic field for $I = 1\ \mu$A. Lower inset shows the SEM image of the sample. Upper inset shows the amplitude of the first resistance peak, ΔR, as a function of temperature (solid dots), compared to the amplitude of the resistance oscillations predicted by the Little-Parks effect, $\Delta R = 0.14(dR/dT)T_c(\xi(0)/(w+a)/4)^2$ [2,15] (open dots). Triangles present the results of the GL simulations. (c) $R(H)$ curves of the sample obtained at $T = 7.42$ K for different values of the bias current.

$\Delta R = 0.14(dR/dT)T_c(\xi(0)/r_{\rm eff})^2$ with $r_{\rm eff} = (w+a)/4$ [2,15]. The LP mechanism predicts resistance oscillations at higher temperatures, $T > 7.5$ K, and can survive until very close to T_c. However, we observed resistance peaks already starting at $T = 7.35$ K and which disappear well below T_c. Moreover, the amplitude of the oscillations reported here is much larger than the ones originating from the LP effect, in spite of the fact that the LP effect is pronounced in low-T_c superconductors due to their relatively large coherence length. On the other hand, current-driven moving vortices can account for the observed large magnetoresistance. The solid curves in Fig. 5(a) are results of theoretical simulations for the parameters of the experimental sample. We found very good agreement with the period of the voltage oscillations, while we observed a weak difference in the amplitude of the oscillations, likely due to the presence of superconducting current and voltage leads in the experiment [see triangles in the top inset of Fig. 5(b)]. In simulations, the damage to the sample near the (hole) edges due to the ion bombardment process (the bright regions in the SEM image of the sample at the sample edges) was modeled by the local suppression of T_c of approx 4% in these regions (~ 20 nm width). We also used the parameter $u = 1$ [see Eq. (1)] to best fit the experimental data, which indicates a larger electric field penetration depth l_E in our experimental samples (since $u \sim l_E^{-2}$) [31]. The interpretation of the voltage oscillations vs magnetic field remains the same as in Figs. 2–4), confirming their origin to be the moving vortices. Here, we must emphasize that due to the small width of the rings [i.e., $(w-a)/2 \lesssim 3\xi(T)$] in the considered temperature range the model of thermally created vortex-antivortex pairs (Ref. [15] and references therein) is not applicable to our experimental sample.

In summary, we have demonstrated that the Little-Parks effect, a landmark manifestation of flux quantization, is not sufficient to fully describe the size and temperature range of typical magnetoresistance oscillations observed in small superconductors. Viable interpretations of such oscillations have been offered in the past by Parks and Mochel [32], Anderson and Dayem [33], Sochnikov *et al.* [15], and Baturina *et al.* [22]. We, however, showed that in low-T_c mesoscopic samples large magnetoresistance oscillations can stem solely from intermittent vortex nucleation, motion, and stabilization by the interplay of the driving current and the persistent Meissner currents in the sample. Furthermore, continuously moving (dissipative) vortices contribute to the background of the magnetoresistance curves, and their contribution grows with increasing field or applied current, an effect not covered by competing explanations. We therefore suggest that, due to ever present current in transport measurements, the contribution of current-induced vortices to dissipation in patterned superconductors can never be entirely disregarded.

This work was supported by the Flemish Science Foundation (FWO-Vl) and the Belgian Science Policy (IAP) (theory) and by the U. S. Department of Energy (DOE) Award No. DE-FG02-06ER46334 (experiment). G. R. B. acknowledges individual grant from FWO-Vl. W. K. K. acknowledges support from DOE BES under Contract No. DE-AC02-06CH11357, which also funds Argonne's Center for Nanoscale Materials (CNM) where the focused-ion-beam milling was performed.

*xiao@anl.gov
†francois.peeters@ua.ac.be

[1] W.-R. Lee and H.-S. Sim, Phys. Rev. Lett. **104**, 196802 (2010).
[2] W. A. Little and R. D. Parks, Phys. Rev. Lett. **9**, 9 (1962); Phys. Rev. **133**, A97 (1964).
[3] M. D. Stewart, Jr., A. Yin, J. M. Xu, and J. M. Valles, Jr., Science **318**, 1273 (2007).
[4] F. Carillo, G. Papari, D. Stornaiuolo, D. Born, D. Montemurro, P. Pingue, F. Beltram, and F. Tafuri, Phys. Rev. B **81**, 054505 (2010).
[5] Yu. S. Erin, S. V. Kuplevakhskii, and A. N. Omel'yanchuk, Low Temp. Phys. **34**, 891 (2008); R. Geurts, M. V. Milošević, and F. M. Peeters, Phys. Rev. B **81**, 214514 (2010).
[6] A. V. Samokhvalov, A. S. Mel'nikov, J.-P. Ader, and A. I. Buzdin, Phys. Rev. B **79**, 174502 (2009); A. Yu. Aladyshkin, D. A. Ryzhov, A. V. Samokhvalov, D. A. Savinov, A. S. Mel'nikov, and V. V. Moshchalkov, *ibid.* **75**, 184519 (2007); M. V. Milošević, S. V. Yampolskii, and F. M. Peeters, Phys. Rev. B **66**, 024515 (2002); M. V. Milošević, G. R. Berdiyorov, and F. M. Peeters, Phys. Rev. Lett. **95**, 147004 (2005); M. V. Milošević and F. M. Peeters, Phys. Rev. Lett. **94**, 227001 (2005); M. V. Milošević and F. M. Peeters, Europhys. Lett. **70**, 670 (2005).
[7] Y. S. Barash, Phys. Rev. Lett. **100**, 177003 (2008); V. Juricic, I. F. Herbut, and Z. Tešanović, *ibid.* **100**, 187006 (2008); G.-Q. Zha, M. V. Milošević, S.-P. Zhou, and F. M. Peeters, Phys. Rev. B **84**, 132501 (2011).
[8] E. Berg, E. Fradkin, and S. A. Kivelson, Nature Phys. **5**, 830 (2009).
[9] R. P. Groff and R. D. Parks, Phys. Rev. **176**, 567 (1968); V. V. Moshchalkov, L. Gielen, M. Dhallé, C. Van Haesendonck, and Y. Bruynseraede, Nature (London) **361**, 617 (1993); V. V. Moshchalkov, L. Gielen, C. Strunk, R. Jonckheere, X. Qiu, C. Van Haesendonck, and Y. Bruynseraede, Nature (London) **373**, 319 (1995); G. R. Berdiyorov, S. H. Yu, Z. L. Xiao, F. M. Peeters, J. Hua, A. Imre, and W. K. Kwok, Phys. Rev. B **80**, 064511 (2009); G. R. Berdiyorov, M. V. Milošević, and F. M. Peeters, Phys. Rev. B **81**, 144511 (2010); J. Bardeen, Phys. Rev. Lett. **7**, 162 (1961); R. M. Arutunian and G. F. Zharkov, J. Low Temp. Phys. **52**, 409 (1983); A. G. Sivakov, A. M. Glukhov, A. N. Omelyanchouk, Y. Koval, P. Müller, and A. V. Ustinov, Phys. Rev. Lett. **91**, 267001 (2003).
[10] H. Vloeberghs, V. V. Moshchalkov, C. Van Haesendonck, R. Jonckheere, and Y. Bruynseraede, Phys. Rev. Lett. **69**, 1268 (1992).
[11] V. Bruyndoncx, L. Van Look, M. Verschuere, and V. V. Moshchalkov, Phys. Rev. B **60**, 10468 (1999); B. J. Baelus, F. M. Peeters, and V. A. Schweigert, Phys. Rev. B **61**, 9734 (2000); M. Morelle, D. S. Golubovic, and V. V. Moshchalkov, Phys. Rev. B **70**, 144528 (2004).
[12] H. J. Fink, A. López, and R. Maynard, Phys. Rev. B **26**, 5237 (1982); R. Rammal, T. C. Lubensky, and G. Toulouse, Phys. Rev. B **27**, 2820 (1983); C. C. Chi, P. Santhanam, and P. E. Blöchl, Phys. Rev. B **42**, 76 (1990); J. I. Castro and A. López, Phys. Rev. B **52**, 7495 (1995); J. Simonin, D. Rodrigues, and A. López, Phys. Rev. Lett. **49**, 944 (1982); O. Sato and M. Kato, Phys. Rev. B **68**, 094509 (2003).
[13] O. Buisson, M. Giroud, and B. Pannetier, Europhys. Lett. **12**, 727 (1990); B. Pannetier, J. Chaussy, R. Rammal, and J. C. Villegier, Phys. Rev. Lett. **53**, 1845 (1984); C. C. Abilio, P. Butaud, T. Fournier, B. Pannetier, J. Vidal, S. Tedesco, and B. Dalzotto, Phys. Rev. Lett. **83**, 5102 (1999); F. Nori and Q. Niu, Physica (Amsterdam) **152B**, 105 (1988); J. M. Gordon, A. M. Goldman, and B. Whitehead, Phys. Rev. Lett. **59**, 2311 (1987); P. L. Gammel, P. A. Polakos, C. E. Rice, L. R. Harriott, and D. J. Bishop, Phys. Rev. B **41**, 2593 (1990); A. Behrooz, M. J. Burns, D. Levine, B. Whitehead, and P. M. Chaikin, Phys. Rev. B **35**, 8396 (1987); U. Patel, Z. L. Xiao, J. Hua, T. Xu, D. Rosenmann, V. Novosad, J. Pearson, U. Welp, W. K. Kwok, and G. W. Crabtree, Phys. Rev. B **76**, 020508 (2007).
[14] J. E. Mooij and G. B. Schon, in *Proceedings of Coherence in Superconducting Networks* (North-Holland, Amsterdam, 1988).
[15] I. Sochnikov, A. Shaulov, Y. Yeshurun, G. Logvenov, and I. Bozovic, Nature Nanotech. **5**, 516 (2010); I. Sochnikov, A. Shaulov, Y. Yeshurun, G. Logvenov, and I. Božović, Phys. Rev. B **82**, 094513 (2010).
[16] J. R. Kirtley, C. C. Tsuei, V. G. Kogan, J. R. Clem, H. Raffy, and Z. Z. Li, Phys. Rev. B **68**, 214505 (2003).
[17] F. London, Phys. Rev. **74**, 562 (1948).
[18] B. S. Deaver, Jr. and W. M. Fairbank, Phys. Rev. Lett. **7**, 43 (1961); R. Doll and M. Näbauer, Phys. Rev. Lett. **7**, 51 (1961).
[19] J. Simonin, D. Rodrigues, and A. López, Phys. Rev. Lett. **49**, 944 (1982); H. J. Fink, A. López, and D. Rodrigues, Jpn. J. Appl. Phys. **26**, L1465 (1987); H. J. Fink, O. Buisson, and B. Pannetier, Phys. Rev. B **43**, 10144 (1991); H. J. Fink and S. B. Haley, Phys. Rev. Lett. **66**, 216 (1991); G. R. Berdiyorov, M. V. Milošević, and F. M. Peeters, Phys. Rev. B **74**, 174512 (2006); G. R. Berdiyorov, M. V. Milošević, and F. M. Peeters, Phys. Rev. Lett. **96**, 207001 (2006).
[20] D. Y. Vodolazov, F. M. Peeters, M. Morelle, and V. V. Moshchalkov, Phys. Rev. B **71**, 184502 (2005).
[21] V. M. Vinokur, T. I. Baturina, M. V. Fistul, A. Yu. Mironov, M. R. Baklanov, and C. Strunk, Nature (London) **452**, 613 (2008).
[22] T. I. Baturina, V. M. Vinokur, A. Yu. Mironov, N. M. Chtchelkatchev, D. A. Nasimov, and A. V. Latyshev, Europhys. Lett. **93**, 47002 (2011).
[23] L. Kramer and R. J. Watts-Tobin, Phys. Rev. Lett. **40**, 1041 (1978); R. J. Watts-Tobin, Y. Krähenbühl and L. Kramer, J. Low Temp. Phys. **42**, 459 (1981).
[24] R. Kato, Y. Enomoto, and S. Maekawa, Phys. Rev. B **47**, 8016 (1993).
[25] T. Winiecki and C. S. Adams, J. Comput. Phys. **179**, 127 (2002); D. Yu. Vodolazov and F. M. Peeters, Phys. Rev. B **76**, 014521 (2007).
[26] V. A. Schweigert and F. M. Peeters, Phys. Rev. B **57**, 13817 (1998).
[27] See Supplemental Material at http://link.aps.org/supplemental/10.1103/PhysRevLett.109.057004 for an online video showing the time evolution of the superconducting order parameter and output voltage in the ladder geometry.
[28] D. Y. Vodolazov, I. L. Maksimov, and E. H. Brandt, Physica (Amsterdam) **384C**, 211 (2003).

[29] J. Hua, Z. L. Xiao, A. Imre, S. H. Yu, U. Patel, L. E. Ocola, R. Divan, A. Koshelev, J. Pearson, U. Welp, and W. K. Kwok, Phys. Rev. Lett. **101**, 077003 (2008).
[30] See Supplemental Material at http://link.aps.org/supplemental/10.1103/PhysRevLett.109.057004 for a figure of magnetoresistance curves of the sample with interhole spacing $d = 300$ nm.
[31] B. I. Ivlev, N. B. Kopnin, and L. A. Maslova, Zh. Eksp. Teor. Fiz. **78**, 1963 (1980) [Sov. Phys. JETP **51**, 986 (1980)].
[32] R. D. Parks and J. M. Mochel, Rev. Mod. Phys. **36**, 284 (1964).
[33] P. W. Anderson and A. H. Dayem, Phys. Rev. Lett. **13**, 195 (1964).